App. Envi. Res. 44(3) (2022): 33-44

Applied Environmental Research

Journal homepage : http://www.tci-thaijo.org/index.php/aer

Disinfection By-product Precursor Removal by Biochar Derived from Agricultural Waste

Sorawit Ritthisoonthorn[1], Yuvarat Ngernyen[2], Lippakorn Songnangrong[1], Warodom Rattanaboonta[1], Watsa Khongnakorn[3], Panitan Jutaporn[1,*]

[1] Research Center for Environmental and Hazardous Substance Management (EHSM), Department of Environmental Engineering, Faculty of Engineering, Khon Kaen University, Khon Kaen, Thailand
[2] Biomass & Bioenergy Research Laboratory, Department of Chemical Engineering, Faculty of Engineering, Khon Kaen University, Khon Kaen, Thailand
[3] Center of Excellence in Membrane Science and Technology, Department of Civil and Environmental Engineering, Faculty of Engineering, Prince of Songkla University, Songkhla, Thailand
[*] Corresponding author: panitju@kku.ac.th

Article History
Submitted: 16 May 2022/ Revision received: 1 July 2022/ Accepted: 10 July 2022/ Published online: 11 August 2022

Abstract

Biochar made from agricultural waste products can be used as a low-cost adsorbent targeting dissolved organic matter (DOM). In water treatment plant (WTP), DOM reacts with chlorine-based disinfectant and forms carcinogenic disinfection by-products. The objective of this study was to investigate the applicability of bamboo biochar derived from wood vinegar production waste as an adsorbent for DOM removal and subsequently trihalomethane formation potential (THM-FP) reduction. Raw biochar (BCRaw) and 800°C post-heated biochar (BC800) was tested for its surface characteristics including scanning electron microscopy, Fourier transform infrared spectroscopy and Brunauer, Emmett and Teller analysis. The post-pyrolysis treatment increased the surface area of the biochar from 90.3 to 274 m^2 g^{-1}. Raw natural water collected from Tapra WTP, Khon Kaen, Thailand, which uses the Chi River as its water source. The adsorption capacities for dissolve organic carbon at 24-h equilibrium (Q_e) of BCRaw and BC800 were 0.148 and 0.551 mg-C g^{-1} adsorbent, respectively. The adsorption kinetics were described well with a pseudo-second order model, which implied chemisorption and multiple adsorption mechanisms. While THM-FP was relatively unaffected by a treatment with BCRaw, a treatment with BC800 resulted in 12.4% THM-FP reduction and preferential removal of precursor to chloroform over other THMs was observed. Fluorescent excitation-emission matric spectroscopy was employed to characterize DOM before and after treatment with biochar. BC800 achieved greater removal of terrestrial humic-like and fulvic-like DOM, due to the presence of oxygen functional groups, which enhances removal capacity for aromatic compounds. Overall, this study shows the potential use of bamboo biochar derived from waste material as an adsorbent for THM precursor removal.

Keywords: Biochar; Adsorption; Dissolved organic matter; Characterization; Trihalomethanes

https://doi.org/10.35762/AER.2022.44.3.3

Introduction

Biochar is a carbon-rich material produced from thermal combustion of carbon-based biomass or agricultural wastes under limited-oxygen conditions. Biochar has been previously applied to soil to sequester carbon and improve soil conditions [1]. Due to its high carbon content, large surface area, and high porosity, biochar is a proven adsorbent effective for removal of various types of pollutants [2]. Biochar has some advantages over commercial activated carbon in its lower production cost, local availability, and environmentally friendly production. The used biochar can be disposed by combustion or gasification to produce energy or subsequently used as a soil amendment, providing sustainable waste management.

Physiochemical properties of biochar (e.g., surface area, pore size, and functional groups) vary with the raw materials and preparation conditions [3]. With a proper pyrolysis temperature and modification process, biochar can be used to target removal of specific contaminants. For environmental applications, biochar has been used as an adsorbent for decontamination of water and wastewater, including removal of dissolved organic matter (DOM) [4–5], DOM and phosphorus [6], toxic metals [7], and emerging contaminants [8].

In water treatment, DOM is a major concern because it causes undesirable taste and odor and can react with chlorine-based disinfectants to form carcinogenic disinfection byproducts (DBPs). In Thailand, water authorities regulate concentration of chloroform (TCM), bromodichloromethane (BDCM), dibromochloromethane (DBCM), and bromoform (TBM) in tap water does not exceed 300, 60, 100, and 100 μg L^{-1}, respectively, and the summation of the ratio of the four THMs to their respective standard does not exceed one [9]. To control DBPs concentration in tap water, water treatment plants (WTPs) use conventional coagulation to remove DOM, organic precursor to DBPs. However, coagulation is more effective at removing turbidity rather than DOM. Coagulation using polyaluminum chloride (PACl) in the full-scale in WTPs in Thailand only achieved 8.9–16% dissolved organic carbon (DOC) removal [10]. Commercial activated carbon (AC) can be used to enhance DOC removal. For the water sampled from Bangkhen WTP, PACl coagulation enhanced with powder activated carbon (PAC) at 20 mg L^{-1} could increase DOC removal by 33% [11].

As biochar has similar characteristics to AC, it has potential to be used as a low-cost adsorbent to replace commercial AC to remove DOM, and thus reduce the risk of DBPs formation at WTPs. Accordingly, the objective of this study was to investigate the applicability of biochar derived from waste material as an adsorbent for DOM removal. We examined surface properties of the raw and post-pyrolysis biochar and the characteristics of DOM before and after treatment with the biochar. The adsorbent performance of biochar was evaluated using surface water sampled from the Chi River, a water source for the Tapra WTP in Khon Kaen, Thailand, where high concentration of THMs in finished water was previously reported.

Materials and method

1) Preparation of biochar

Bamboo biochar was prepared from wasted char, a byproduct from a wood vinegar manufacturing process (Ubon Ratchathani, Thailand). During the wood vinegar production, the bamboo wood (approximately 2 m long) was carbonized at 1200°C under limited oxygen for 15 days [8]. The released gases were condensed (cooled) into a liquid, then the liquid was further refined into wood vinegar. The char that was left after pyrolysis is considered agricultural byproduct with only marginal economic value. Thus, the waste-derived biochar may be a potential low-cost adsorbent material, thereby supporting agricultural waste utilization.

The wasted char was crushed and sieved into 2–4 mm in size, washed with deionized (DI) water, and dried at 105°C in an oven overnight. Then, the raw biochar was loaded into packed-bed reactor made from stainless steel (5 × 30 cm) and then pyrolyzed in a vertical electric furnace under nitrogen (N_2) flow of 250 cm^3 min^{-1} at 800°C for 1 h with heating rate 20 °C min^{-1} to remove organic residuals. The in-house pyrolysis furnace was previously used to carbonized agricultural materials to produce biochar and activated carbon in previous studies [12–13]. The sample was left to cool down to room temperature under the N_2 atmosphere. The raw and post-pyrolysis biochar samples were named BCRaw and BC800, respectively. All the ad-sorbents were kept in an air-lock container at room temperature until use.

2) Characterization of biochar

The biochar samples were characterized for their morphology and surface characteristics using field emission scanning electron microscopy (SEM, Helios NanoLab G3 CX, FEI). The functional groups on all biochar samples were identified using Fourier transform infrared spectroscopy (FTIR, TENSOR27, Bruker) in spectra ranging from 400 to 4000 cm^{-1}. The Brunauer, Emmett and Teller (BET) specific surface area, pore size, and pore volume of biochar was evaluated from N_2 adsorption–desorption isotherms (BET, ASAP 2460, micromeritics).

3) Removal of DOM by biochar

Adsorption batch experiments were conducted to evaluate the DOM removal performance of the biochar. In Feb 2022, water samples were collected from an intake of Tapra WTP, Khon Kaen, Thailand, which used the Chi River as a source water. Upon arrival at a laboratory, the water samples were filtered with 0.7 µm glass fiber filter (GF/F, Whatman) to remove suspended solids, and then stored at 4°C in the dark until needed. Water samples were allowed to reach room temperature (28±2°C) before the batch experiments. The DOM removal experiments were conducted at room temperature (28±2°C) by adding 3 g of biochar into 1 L of raw water and mixing at 150 rpm for 24 h [4]. Samples were collected periodically from 0–1440 min. The used biochar was then separated from the treated water using a stainless-steel fine screen. The treated water samples were filtered again with a 0.7-µm GF/F filter before organic matter characterization. DOC was analyzed using multi N/C® 2100 TOC Analyzer (Analytik Jena AG, Germany). UV absorbance was made using a 1-cm quartz cell and DR600 spectrophotometry (Hach, USA). Specific UV absorbance (SUVA) was calculated as a ratio of UV absorbance at 254 nm (UV254) and the DOC concentration. SUVA values are used as an indicator of the aromaticity of DOM in the samples [14]. The batch experiments were conducted in duplicate and water quality analyses were performed in replicated. A Mann-Whitney test or a pairwise t-test was conducted to compare the differences between the water treated by BCRaw and BC800. All statistical analyses were done using Stata IC 13.1 (Stata Corp LP, College Station, TX, USA).

The adsorption capacity of biochar at equilibrium (Qe, mg g^{-1}) can be determined the following Eq. 1 [15].

$$Q_e = \frac{(C_0 - C_e)}{m} V \qquad \text{(Eq. 1)}$$

when C_0 (mg L^{-1}) and C_e (mg L^{-1}) correspond to the DOC concentration at time zero and at equilibrium, respectively. V (L) corresponds to the volume of the water tested and m (g) is the mass of the biochar used. The experimental data was then fit to the pseudo-first-order (PFO) and pseudo-second-order (PSO) models to explain adsorption kinetics following Eq. 2 and 3, respectively, where Q_t (mg g^{-1}) is the adsorption capacities at time t. k_1 (min^{-1}) and k_2 (g (mg

$min^{-1})^{-1}$) are the rate constants of the PFO and PSO models, respectively [13].

$$\ln(Q_e - Q_t) = \ln Q_e - k_1 t \quad \text{(Eq. 2)}$$

$$\frac{t}{Q_t} = \frac{1}{k_2 Q_e^2} + \frac{1}{Q_e t} \quad \text{(Eq. 3)}$$

Fluorescent excitation-emission matrix (EEM) spectroscopy was employed to track changes in the composition of DOM fractions before and after treatment with biochars. EEM spectra were collected using a spectrofluorometer with a Xenon arc lamp and a PMT detector (FS5, Edinburgh) and a 1-cm quartz cell according to a procedure reported in a previous study [16]. EEMs were generated from excitation wavelengths from 200 to 500 nm with 5-nm increments, and the emission was recorded in the range of 250 to 550 nm with 1-nm increment. Blank EEM from DI water was collected on the same day prior to sample scan. Sample EEMs were corrected for inner filtering effects using a matrix generated from UV-vis spectra [17]. UV absorbance measurement was made using 1-cm quartz cell and a spectrophotometer (DR6000, Hach). Sample EEMs were then blank-subtracted, and the fluorescence intensities were normalized to the area under the water-Raman peak at an excitation of 350 nm [16]. Thus, EEM data is reported in Raman units.

4) DBPs analysis

Raw and biochar-treated water chlorinated using sodium hypochlorite (NaOCl) solution according to the uniform formation conditions (UFC) method [18]. The UFC is used to represent the real chlorine concentration in the distribution system, which refers to concentration of chlorine that yields 1.0 mg-Cl L^{-1} residual after 24-h incubation at pH 8 at 20ºC in the dark. The NaOCl solution was added to the samples using the ratio of carbon to chlorine from 1:1 to 1:2, and sample with chlorine residual of 1.0±0.2 mg L^{-1} were selected for THMs analysis. Four THMs, including CF, BDCM, DBCM, BF, were analyzed by liquid/liquid extraction according to EPA method 551.1 using gas chromatography-electron capture detector (GC-ECD, Shimadzu Nexis GC - 2030, Japan) with Rtx®-5 column. Methyl *tert* butyl ether (MtBE) was used as extracting solvent and ammonium chloride (NH_4Cl) was used as a dechlorinating agent.

Results and discussions

1) Characteristics of the adsorbents

Based on SEM images, the micropores and mesopores of the biochars were observed, and the surface of BC800 (Figure 1b) was more porous compared to that of BCRaw (Figure 1a). Thus, pyrolysis of the previously crushed and sieved biochar successfully increased its porosity. Compared to BCRaw, thermal activation resulted in a substantial decrease in several functional groups on BC800 (Figure 1c), denoted by the FTIR troughs around 3000 cm^{-1} (CH_2 stretching vibrations for aliphatic groups), 1410 cm^{-1} (aromatic skeletal stretching bands, presence of lignin), 1250–1050 cm^{-1} (C–O–C stretching for cellulose and hemicellulose), 872 cm^{-1} (aromatic, C=H out of plane bending or Si-O-Si bond bending vibrations), and 600–700 cm^{-1} (C–H bond in aromatic and heteroatomic compounds) [4, 19–21]. The bands between 2850–3000 cm^{-1} showed -OH functional group on BCRaw [20], which decreased due to thermal conversion of aromatic lignin and alcohol [22]. This was attributed to the decrease in the polar functional groups after pyrolysis, thus confirming the decomposition of hemicellulose and conversion to graphitic structure of biochar. Similar phenomena have been previously reported in preparation of activated biochars from eucalyptus and bamboo wood [4, 20]. The FTIR troughs around 2068–2100 cm^{-1}, which correspond to C≡C stretching [4, 6], were relatively unchanged after pyrolysis. The band between 1100–1000 cm^{-1} (C-O-C stretch of the ethers present in lignin) [23] was still present in BC800 but at a

less prominent level. The higher retained amount of oxygen functional groups, e.g., anhydride (CO-O-CO stretching, 1045 cm^{-1}) on the surface of BC800 indicated the presence of aromatic functionality [24], which is an important factor for adsorption capacity of organic materials.

The development of mesoporous and microporous structures for the BC800 is further confirmed by BET- specific surface area, pore volume, and pore size (Table 1). BCRaw has a lower surface area of 90.35 m^2 g^{-1} and pore volume of 0.046 cm^3 g^{-1}. The low surface area was caused by the presence of cellulose, lignin, tar and other organic materials in the tight structure of the initial waste char, as the wood vinegar production typically uses large pieces of bamboo timber as raw materials. Thus, the heat distribution and gasification were not effective. Following pyrolysis at 800°C, the surface area and pore volume of BC800 increased to 274.4 m^2 g^{-1} and 0.140, cm^3 g^{-1}, respectively. The average pore size of BC800 (2.002 nm) was slightly smaller than that of BCRaw (2.076 nm). Thus, compared to BCRaw, pyrolysis resulted in an increase of surface area and pore volume, while the impact on average pore size was marginal.

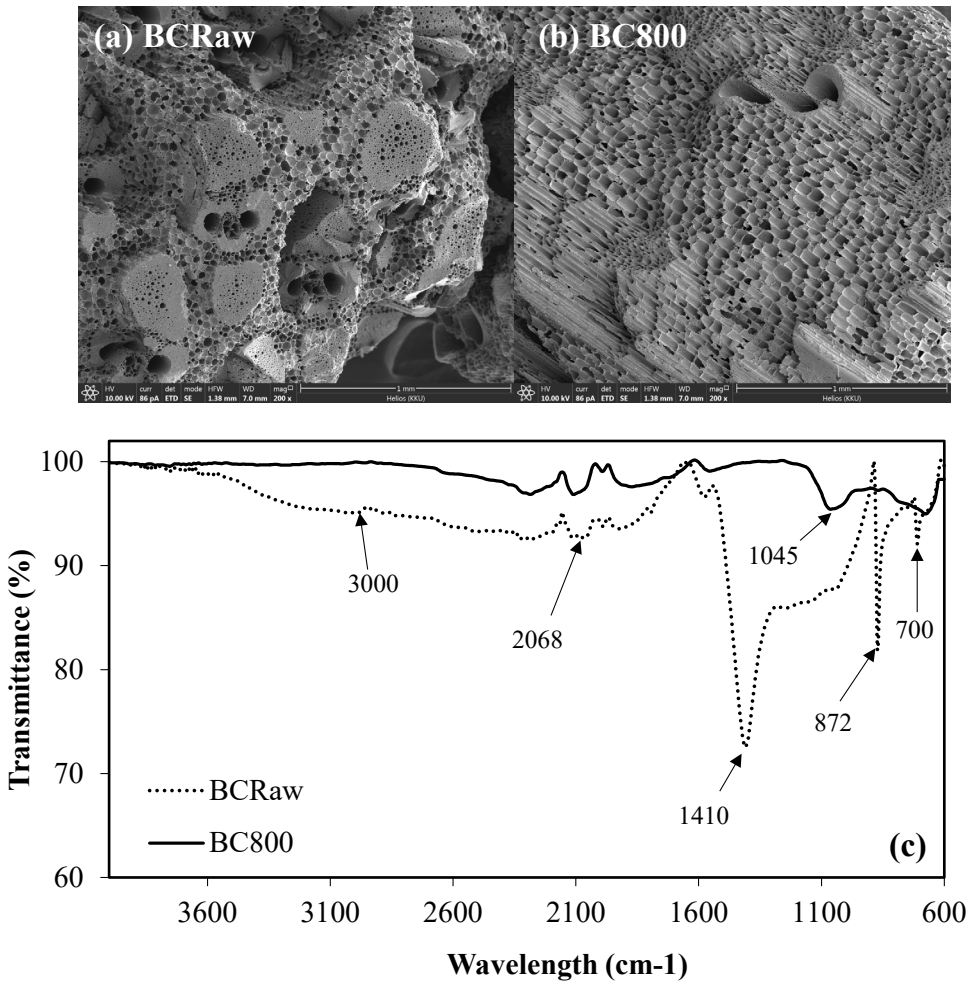

Figure 1 SEM images of (a) BCRaw and (b) BC800 and (c) FTIR spectra.

Table 1 Surface properties of the biochar samples

Samples	BET Surface area (m^2 g^{-1})	Pore volume (cm^3 g^{-1})	Pore size (nm)
BCRaw	90.35	0.046	2.076
BC800	274.4	0.140	2.002

The shape of N_2 adsorption–desorption isotherms describe a type II isotherm, which indicates adsorption with strong interactions within wide range of pore sizes (Figure 2). Such adsorption may extend from the monolayer to the multilayer. Notably, the hysteresis remained unclosed at lower relative pressure region, similar to a previous study [25], which was explained as slow desorption of the adsorbed N_2 at low pressure due to strong chemisorption and capillary condensation phenomenon.

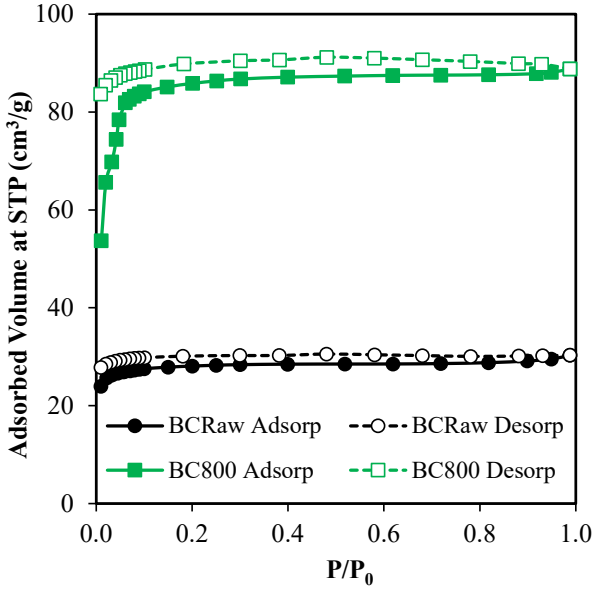

Figure 2 Nitrogen adsorption-desorption isotherms of the biochar.

2) Adsorption of DOM by biochar

The raw water from Chi River had a DOC concentration of 4.21 mg L^{-1} and UV254 of 0.093 cm^{-1}, resulting in a SUVA value of 2.21 L $mg^{-1}m^{-1}$. After equilibrating for 24 h, DOC removal by BCRaw and BC800, was 14.7 and 37.8%, respectively (Figure 3a). During 15–1440 min of the DOC removal experiment, DOC of the water treated by BC800 was significantly lower than that treated by BCRaw (Mann-Whitney test, $p < 0.05$). DOC removal by BC800 was greater than that achieved by PACl coagulation at Tapra WTP (8.9–16%) during 2018–2019 [10]. Previous studies have tested various types of biochar and commercial activated carbon (AC) to remove DOM from natural surface water. Pinecone biomass-derived biochar resulted in less than <25% DOM removal from lake water, while biochar with alkali activation improved the DOM removal to > 80% [25]. The other study using river water with a DOC of 4.13 mg L^{-1} reporting that commercial coconut shell-based AC achieved 49.64% DOC removal [4]. The metal-impregnated biochars derived from softwood sawdust in the range of 0.5–2 g L^{-1} could remove 87–96% of DOM [6]. Thus, BC800 has greater DOM removal efficiency compared to other pristine biochar and not far behind compared to commercial AC, and future study should focus on alkali activation and metal-impregnation to improve DOM removal efficiency of biochar.

Treatment by BCRaw significantly increased SUVA value of the raw water from 2.21 L mg^{-1} m^{-1} to 2.42 L $mg^{-1}m^{-1}$ (t-test. $p < 0.05$), respectively, suggesting preferential removal of a non-UV absorbing DOM by BCRaw. The adsorption capacity at equilibrium (Q_e) of BCRaw and BC800 was 0.148 and 0.551 mg g^{-1} adsorbent, respectively (Figure 3b). Compared to BCRaw, the greater DOC removal by BC800 is consistent with its higher surface area and pore volume (Table 1). Additionally, the adsorption kinetics of BCRaw and BC800 for DOC were fitted with PSO model ($R^2 = 0.99$) with a rate constants k_2 of 0.193 g mg-C^{-1}·min^{-1} for BCRaw and 0.017 g mg-C^{-1}·min^{-1} for BC800. Fitting DOC removal data with the PFO model resulted in R^2 of 0.77 and 0.96 for BCraw and BC800, respectively. A previous study [4] also reported that the PSO model better fit well the adsorption kinetics of organic pollutants by biochar compared to the PFO model. The PSO model implied chemisorption and multiple adsorption mechanisms and that chemical adsorption was considered as the rate-limiting step of DOC adsorption on the biochar.

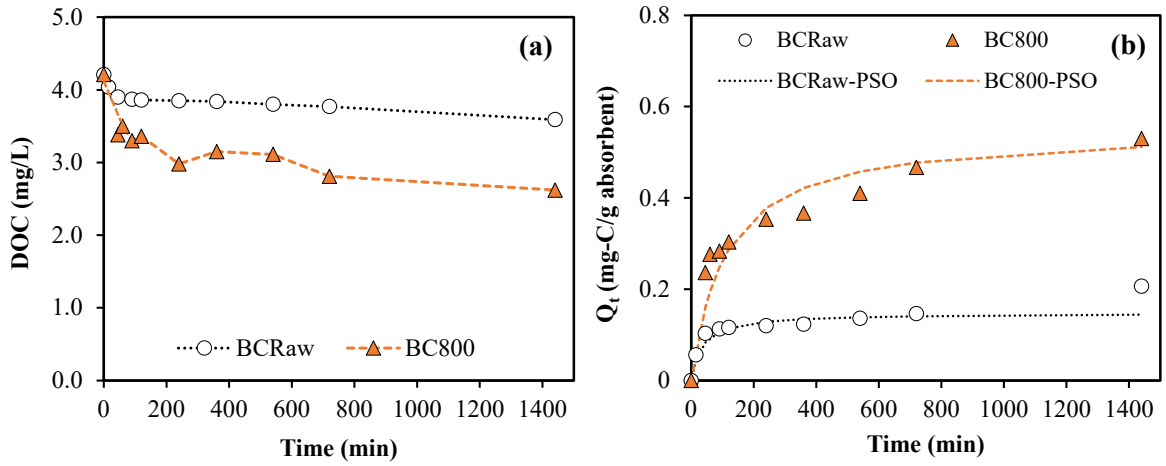

Figure 3 (a) Reduction of DOC by 3 g L^{-1} biochar over time and (b) adsorption capacity (Q_t) of biochar. Lines indicated ideal reduction of DOC by pseudo second-order reaction.

Using the peak-picking characterization technique, fluorescence EEM contours revealed four distinguished peaks in the water samples (Figure 4). The four peaks are designated as letters A, C, T and B based on previous work [26]. According to their excitation/emission coordinates, peak A (250 nm/450 nm), peak C (315 nm/415 nm), peak T (275 nm/340 nm), and peak B (230 nm /300 nm) can be classified as terrestrial fulvic-like, terrestrial humic-like, tryptophan protein-like, and tyrosine protein-like DOM, respectively. The raw water (Figure 4a) was enriched in terrestrial DOM (peaks A and C) and the EEM contour shows greater fluorescence intensities at all peak locations compared to water treated with BCRaw and BC800 (Figure 4b and 4c).

For quantitative comparison, the fluorescence intensity at peaks A, C, T, and B for all raw and biochar-treated water is presented in Figure 5a. Pairwise t-test was used to compare the fluorescence intensity of BCRaw-treated and BC800-treated samples (n = 6 from duplicate experiments and replicate measurement). The results show that fluorescence intensity at peaks A, C, and T of BC800-treated sample was significantly lower than those in BCRaw-treated sample (p<0.05 for all three peaks. There was no significant difference (p>0.05) between the fluorescence intensity at peak T of BCRaw-treated and BC800-treated samples. Thus, BC800 achieved greater removal of DOM at peaks A, C, and T (47–65%, Figure 5b) compared to BCRaw (11–35%, Figure 5b), while the removal of DOM at peak B was slightly lower (36% compared to 51%). However, the decline in removal efficiency of DOM at peak B was not significant due to the low fluorescence intensity at peak B in the raw water sample. The greater removal of fluorescence DOM by BC800 was consistent with the greater DOC removal results from kinetics study. Moreover, the greater removal of terrestrial humic-like and fulvic-like DOM by BC800 is well supported by FTIR results reporting that BC800 contains oxygen functional group, e.g., anhydride (CO-O-CO stretching), which enhances adsorption capacity for aromatic compounds.

3) Formation potential and speciation of THMs

Concentration and speciation of the four THMs formed after chlorine was added to the raw and biochar-treated water is shown in Figure 6. The THM formation potential (THM-FP) of the raw water was 188 µg L^{-1}, with TCM and BDCM accounted for 34.8% and 31.7% of the total THM-FP, respectively. Concentration of bromide (Br) in the raw water is 0.6 mg L^{-1} , which is considered very high for surface water

and the presence of brominated DBPs in the finished water was previously reported [9–10] During chlorine disinfection process, Br can be oxidized to hypobromous acid (HOBr) by hypochlorousacid (HOCl). Compared to HOCl, HOBr is a stronger oxidizing agent with greater halogenating activity [27] Thus, the presence of Br promotes formation of brominated DBPs, which has greater toxicity than their corresponding chlorinated DBPs [29\8].

Despite its DOC removal of 14.7%, THM-FP reduction by BCRaw was only marginal (1.5%) (Figure 6). This result agrees well with the increase of SUVA and the low removal of fluorescence DOM at peak A and C by BCRaw treatment, which indicates that BCRaw did not well adsorb UV absorbing material or humic-like fraction of DOM pool that are an important precursor of THMs. For BC800, THM-FP reduction was 12.4%. Preferential removal for FP of TCM (43.7%) and BDCM (20.1%) was observed, while FP of DBCM and TBM increased after BC800 treatment. This result suggests that, for the raw water containing bromide, DOM not removed by BC800 was more susceptible for oxidation by HOBr, led to formation of brominated THMs. Thus, for WTPs using raw water containing high levels of both DOC and Br, other treatment process should also be considered for inorganic precursor removal. Since humic materials are an important precursor of many DBPs, the greater removal of humic-like DOM by BC800 (Figure 5b) explains its capability of THM-FP reduction (Figure 6).

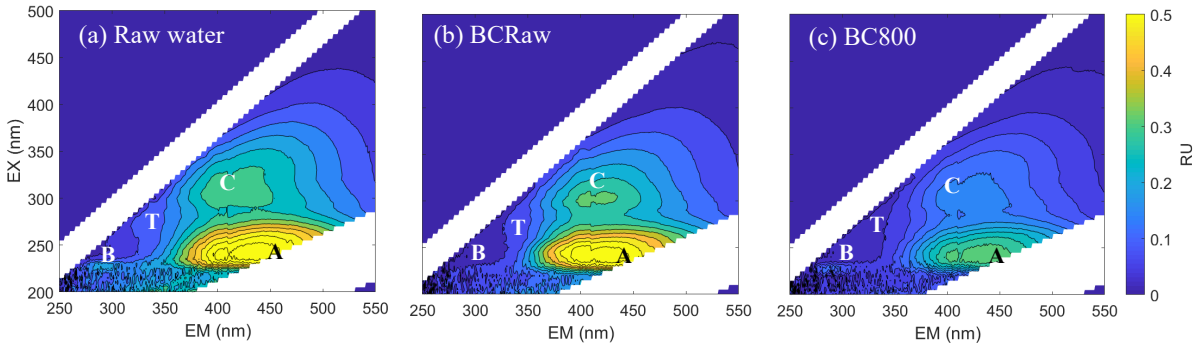

Figure 4 Fluorescence excitation-emission matrix (EEM) contour of (a) raw water, (b) BCRaw-treated water, and (c) BC800-treated water. Peaks A, C, T and B correspond to fulvic-like, humic-like, tryptophan-like, and tyrosine-like DOM, respectively.

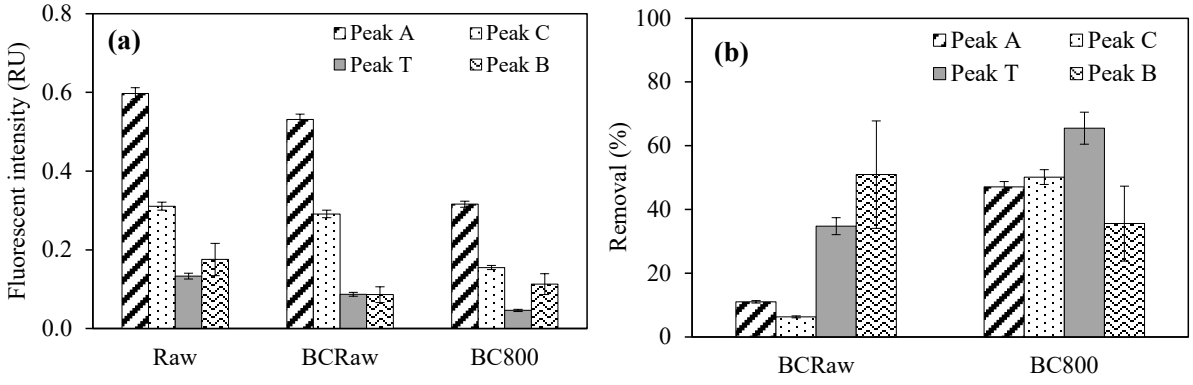

Figure 5 (a) Fluorescence intensity of the raw and treated water, (b) reduction of fluorescence intensity by 3 g L^{-1} BCRaw and BC800 at 24-h contact time. Error bars correspond to the standard deviation of results obtained from duplicate experiment and triplicate measurements. Pairwise t-test was used for statistical analysis to compare the difference between two groups of samples.

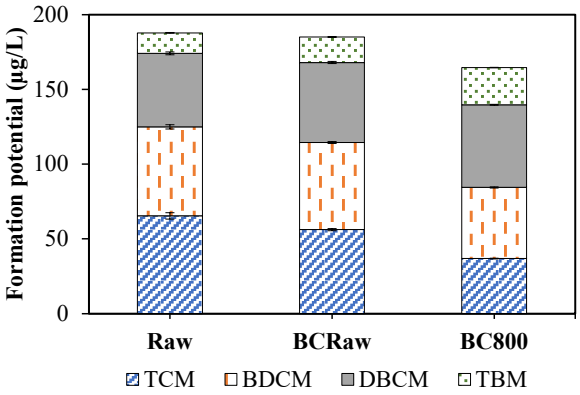

Figure 6 Formation potential of chloroform (TCM), bromodichloromethane (BDCM), dibromochloromethane (DBCM), and bromoform (TBM) in raw and 3 g L^{-1} biochar-treated water.

4) Application of waste-derived biochar for water treatment

Many studies referred to biochar as a low-cost adsorbent compared to activated carbon [4, 6, 29–30]. Cost of biochar production from forest chips includes cost of timber, cost of cutting, chipping, and overheads, road transportation cost, production stage cost. Additional cleaning cost may be required as well [29]. In this study, waste char was used as raw material for biochar production, thus, no cost of timber is required. Since the wood vinegar production use bamboo wood of 2 m, cost of cutting and shipping is required to produce smaller pieces of biochar for homogenous surface properties. Consider the electricity cost for the small furnace (150 kWh) and high grade N_2 gas use in this study, production of biochar in a small lab-scale is not economical. However, if the production is enlarged to a full-scale, waste heat from wood vinegar production or other near-by processes can be used to post-heat the chipped biochar. Thus, transportation cost and production stage cost can be minimized.

In this study, we used DI water to rinse and remove background DOC from biochar follow procedure published in previous studies [4] as background DOC could interfere with DOM characterization. For a full-scale application in WTPs, biochar can be installed to retrofit existing media filtration tank, similar to granular activated carbon filtration. After backwashing, the media filter is typically rinsed with raw water (no cost) in the ripening period, thus DI rinsing is not necessary. In Thailand, the price of charcoal is about \$0.5–1.0 kg^{-1} and activated carbon market price was in the range of \$3–5 kg^{-1}, so production of biochar from waste char can provide value added to the wood vinegar production. The mean price of biochar in global market is \$2.65 kg^{-1}. The price of biochar can be as low as \$0.09 kg^{-1} in the Philippines while the price in the UK is \$8.85 kg^{-1} [29]. Based on the results, BC800 or post-pyrolysis bamboo biochar successfully remove DOC and THM-FP from the raw water. Post-pyrolysis without chemical activation also is cost effective and environmental-friendly, which make it more suitable for application in water treatment.

Conclusion

This study investigated the performance of biochar derived from wood vinegar manufacturing waste in removing DOM and THMs precursors from surface water. Compared to raw biochar, crushing, screening, and post-pyrolysis under N_2 atmosphere at 800°C for 1 h significantly increased surface area of the biochar from 90.35 to 274.4 m^2 g^{-1}. Characterization analyses e.g. BET, SEM, and FTIR revealed mesoporous structure, increase in surface area, larger pore volume and aromatic functional groups on the surface of the post-pyrolysis biochar, for which enhanced its adsorbent capability for DOM and THM-FP removal. Fluorescence EEM characterization revealed that the post-pyrolysis biochar had greater removal of humic materials. Overall, the results from biochar surface chemistry analysis, DOM adsorption study, DOM characterization, and THM-FP evaluation confirm the potential to use this biochar in DOM removal.

The BET surface area of BC800 (274.4 $m^2 g^{-1}$), however, was still less than commercial coal-based activated carbon. Thus, future work should focus on biochar activation using chemical activators to improve the surface chemistry and tailor the modification process to produce biochar as selective adsorbents for DBP precursor removal. This study proposes a value-added alternative for waste char from agricultural production and a biochar that has a potential to be used as an adsorbent for DOM removal.

Acknowledgement

The authors would like to acknowledge financial support from the Research Center for Environmental and Hazardous Substance Management (EHSM), Khon Kaen University, Thailand, and National Research Council of Thailand (NRCT) and The National Science and Technology Development Agency (NSTDA). We also thank our collaborators at water treatment plants who facilitated water sample collection.

References

[1] Verheijen, F., Jeffery, S., Bastos, A.C., Van Der Velde, M., Diafas, I. Biochar application to soils: A critical scientific review of effects on soil properties, Processes and Functions, 2010.

[2] Malik, D.S., Jain, C.K., Yadav, A.K., Banerjee, S. Role of plant-based biochar in pollutant removal: An overview, in Advanced Materials for Waste Water Treatment. Scrivener Publishing LLC, 2017, 313–330.

[3] Wang, J., Wang, S. Preparation, modification and environmental application of biochar: A review. Journal of Cleaner Production, 2019, 227, 1002–1022.

[4] Phinyothanmakorn, N., Prasert, T., Ngernyen, Y., Siripattanakul-Ratpukdi, S., Phungsai, P. Characterization of molecular dissolved organic matter removed by modified eucalyptus-based biochar and disinfection by-product formation potential using Orbitrap mass spectrometric analysis. Science of the Total Environment, 2022, 820, 153299.

[5] Menya, E., Olupot, P.W., Storz, H., Lubwama, M., Kiros, Y. Production and performance of activated carbon from rice husks for removal of natural organic matter from water: A review. Chemical Engineering Research and Design, 2018, 129, 271–296.

[6] Tomin, O., Vahala, R., Yazdani, M.R. Tailoring metal-impregnated biochars for selective removal of natural organic matter and dissolved phosphorus from the aqueous phase. Microporous and Mesoporous Materials, 2021, 328, 111499.

[7] Mohan, D., Kumar, H., Sarswat, A., Alexandre-Franco, M., Pittman, C.U. Cadmium and lead remediation using magnetic oak wood and oak bark fast pyrolysis bio-chars. Chemical Engineering Journal, 2014, 236, 513–528.

[8] Jenjaiwit, S., Supanchaiyamat, N., Hunt, A.J., Ngernyen, Y., Ratpukdi, T., Siripattanakul-Ratpukdi, S. Removal of triclocarban from treated wastewater using cell-immobilized biochar as a sustainable water treatment technology. Journal of Cleaner Production, 2021, 320, 128919.

[9] Ratpukdi, T., Sinorak, S., Kiattisaksiri, P., Punyapalakul, P., Siripattanakul-Ratpukdi, S. Occurrence of trihalomethanes and haloacetonitriles in water distribution networks of Khon Kaen municipality, Thailand. Water Supply, 2019, 19(6), 1–10.

[10] Jutaporn, P., Laolertworakul, W., Tungsudjawong, K., Khongnakorn, W., Leungprasert, S. Parallel factor analysis of fluorescence excitation emissions to identify seasonal and watershed differences in trihalomethane precursors. Chemosphere, 2021, 282(June), 131061.

[11] Tongchang, P., Kumsuvan, J., Phatthalung, W.N., Suksaroj, C., Wongrueng, A., Musikavong, C. Reduction by enhanced coagulation of dissolved organic nitrogen as a precursor of N-nitrosodimethylamine. Journal of Environmental Science and Health - Part A Toxic/Hazardous Substances and Environmental Engineering, 2018, 53(6), 583–593.

[12] Patawat, C., Silakate, K., Chuan-Udom, S., Supanchaiyamat, N., Hunt, A.J., Ngernyen, Y. Preparation of activated carbon from Dipterocarpus alatusfruit and its application for methylene blue adsorption. RSC Advances, 2020, 10(36), 21082–21091.

[13] Youngwilai, A., Kidkhunthod, P., Jearanaikoon, N., Chaiprapa, J., Supanchaiyamat, N., Hunt, A.J., ..., Siripattanakul-Ratpukdi, S. Simultaneous manganese adsorption and biotransformation by Streptomyces violarus strain SBP1 cell-immobilized biochar. Science of the Total Environment, 2020, 713, 136708.

[14] Weishaar, J.L., Aiken, G.R., Bergamaschi, B.A., Fram, M.S., Fujii, R., Mopper, K. Evaluation of specific ultraviolet absorbance as an indicator of the chemical composition and reactivity of dissolved organic carbon. Environmental Science and Technology, 2003, 37(20), 4702–4708.

[15] Tien, C. Adsorption Equilibrium Relationships, isotherm expressions, their determinations, and predictions. Elsevier, 2019.

[16] Poojamnong, K., Tungsudjawong, K., Khongnakorn, W., Jutaporn, P. Characterization of reversible and irreversible foulants in membrane bioreactor (MBR) for eucalyptus pulp and paper mill wastewater treatment using fluorescence regional integration. Journal of Environmental Chemical Engineering, 2020, 8(5), 104231.

[17] Ohno, T. Fluorescence inner-filtering correction for determining the humification index of dissolved organic matter. Environmental Science & Technology, 2002, 36(4), 742–746.

[18] Summers, R.S., Hooper, S.M., Shukairy, H.M., Solarik, G., Owen, D. Assessing DBP yield: Uniform formation conditions. Journal of American Water Works Association, 1996, 88(6), 80–93.

[19] Apaydin-Varol, E., Pütün, A.E. Preparation and characterization of pyrolytic chars from different biomass samples. Journal of Analytical and Applied Pyrolysis, 2012, 98, 29–36.

[20] Sahoo, S.S., Vijay, V.K., Chandra, R., Kumar, H. Production and characterization of biochar produced from slow pyrolysis of pigeon pea stalk and bamboo. Cleaner Engineering and Technology, 2021, 3, 100101.

[21] Taheran, M., Naghdi, M., Brar, S.K., Knystautas, E.J., Verma, M., Ramirez, A.A., ..., Valero, J.R. Adsorption study of environmentally relevant concentrations of chlortetracycline on pinewood biochar. Science of the Total Environment, 2016, 571, 772–777.

[22] Wu, X., Ba, Y., Wang, X., Niu, M., Fang, K. Evolved gas analysis and slow pyrolysis mechanism of bamboo by thermogravimetric analysis, Fourier transform infrared spectroscopy and gas chromatography-mass spectrometry. Bioresource Technology, 2018, 266(June), 407–412.

[23] Pattnaik, D., Kumar, S., Bhuyan, S.K., Mishra, S.C. Effect of carbonization temperatures on biochar formation of bamboo leaves. *In*: IOP Conference Series: Materials Science and Engineering, 2018, 338, 012054.

[24] Huff, M.D., Kumar, S., Lee, J.W. Comparative analysis of pinewood, peanut shell, and bamboo biomass derived biochars produced via hydrothermal conver-Fsion and pyrolysis. Journal of Environmental Management, 2014, 146, 303–308.

[25] Yazdani, M.R., Tailored mesoporous biochar sorbents from pinecone biomass for the adsorption of natural organic matter from lake water. Journal of Molecular Liquids, 2019, 291, 111248.

[26] Coble, P.G., del Castillo, C.E., Avril, B. Distribution and optical properties of CDOM in the Arabian Sea during the 1995 Southwest Monsoon. Deep-Sea Research Part II: Topical Studies in Oceanography, 1998, 45, 2195–2223.

[27] Tian, C., Liu, R., Guo, T., Liu, H., Luo, Q., Qu, J. Chlorination and chloramination of high-bromide natural water: DBPs species transformation. Separation and Purification Technology, 2013, 102, 86–93.

[28] Sharma, V.K., Zboril, R., McDonald, T.J. Formation and toxicity of brominated disinfection byproducts during chlorination and chloramination of water: A review. Journal of Environmental Science and Health - Part B Pesticides, Food Contaminants, and Agricultural Wastes, 2014, 49(3), 212–228.

[29] Ahmed, M.B., Zhou, J.L., Ngo, H.H., Guo, W. Insight into biochar properties and its cost analysis. Biomass and Bioenergy, 2016, 84, 76–86.

[30] Youngwilai, A., Phungsai, P., Supanchaiyamat, N., Hunt, A.J., Ngernyen, Y., Ratpukdi, T., ..., Siripattanakul-Ratpukdi, S. Characterization of dissolved organic carbon and disinfection by-products in biochar filter leachate using orbitrap mass spectrometry. Journal of Hazardous Materials, 2022, 424, 127691.